The influence of notching and mixed-adhesives at the bonding area on the strength and stress distribution of dissimilar single-lap joints

Armin Yousefi Kanani[a], Xiaonan Hou[a*],Jianqiao Ye[a]

[a] Department of Engineering, Engineering Building, Lancaster University, Lancaster, LA1 4YW, UK

[*] Corresponding author (email address: x.hou2@lancaster.ac.uk)

Abstract:

With the rapid development of new engineering materials, multi-material structures are now widely used to achieve desired performances instead of conventional ones**.** The increased use of dissimilar adherends such as composites and metals for joining structural parts in aerospace, maritime and civil and transport structures in the past decades make it essential to find methods to improve the performance of this type of joints due to the potential for lightweight products. The first aim of this research is to minimise peak stress concentration by introducing notches in the bonding area to increase the performance of single-lap joints with epoxy adhesive. This is done by utilising the finite element method (FEA) in Abaqus® software to model a series of single lap joints (SLJ) with various notch designs to find the optimum. Experimental tests are carried out to verify the designs.

The optimal design is used then to model various SLJs with mono-adhesive and mixed-adhesives to optimise single-lap joints with dissimilar adherends. The novel geometrical modification reduces peak stresses significantly in the joints with dissimilar adherends, which leads to smaller asymmetric stress distribution along bond-line. The experimental results show significant improvement in the dissimilar joint strength. Compared with using a single material as the adhesive, it is found that using both epoxy and polyurethane as adhesive offers a higher failure load. This can be explained as the polyurethane adhesive provides more uniform stress distribution by transferring stress concentration to the interior part of the overlap length.

Keywords: Single-lap joint; mixed-adhesives; notches; dissimilar adherends

1. Introduction

Single-lap joints (SLJs) are amongst the most studied and commonly used designs in various engineering applications due to their lower cost and simplicity. Single-lap joints can tolerate significant bending due to the non-collinear load path, which, however, makes it complex to analyse. The eccentric loading condition and differential deformation effects are responsible for the higher peel and shear stresses at the overlap edges where cracks are more likely to be initiated due to the higher stress concentration [1]–[4]. Various joint configurations provide lower stress concentrations at the overlap edges such as a scarf, stepped, and double lap joints, but they are more complicated and expensive to manufacture. Therefore, Single-lap joints have received considerably more attention by researchers to develop novel approaches to reduce stresses at the ends of overlap. Several techniques have been suggested [5-19] to increase the overall strength of the SLJ that can be categorised into two major groups: geometrical and material modifications.

Geometrical modification attempts to change the shape of adherends or adhesives such as adhesive fillet at the edges, tapering, and edge rounding of adherends and notching. Utilising adhesive fillet at the overlap edges create smoother load transmission along the bond-line, leading to lower stress concentration at the edges [5]. Adam et al. [6] studied the effect of fillets or chamfers in the inner and outer adherends, both analytically and experimentally. Numerical and experimental studies were also conducted by Sancaktar and Nirantar [7] to evaluate the influence of geometric changes on peak stresses. They concluded that adherends tapering reduces peel and shear stresses significantly at the overlap edges, resulting in a higher strength of a single-lap joint. McLaren and MacInnes [8] used a different method by bending adherends at the bonding edges to uniform the adhesive stresses along the overlap by eliminating joint eccentricity. Campilho et al. [9] have studied various degrees of eccentricity to optimise joint strength of single-lap joints bonded with brittle and ductile adhesives. Their experimental and numerical results showed that the joint with brittle adhesive experienced better improvement compared to the joints with ductile adhesive as ductile adhesives redistributed stresses in the bonding area, which made them less sensitive to the peak stresses at the overlap edges. Cognard et al. [10] investigated the effect of notches numerically on the peak stresses at the bond-line edges. Their results showed a considerable reduction in stress concentration at the free edges of the adhesive. Sancaktar and Simmons [11] used notches at the end of the bonding region of the top and bottom adherends made of aluminium. Their results presented a 66% and a 3% reduction in peak peel and shear stresses that result in an 8% increase in the experimental joint strength. The work of Yan et al. [12] addressed the effect of length and depth of the notches at the mid-section of the bond-line on both adherends. Their results suggested using large lengths and depths for notches to reduce peak stresses at the overlap edges. Pinto et al. [13] investigated the effect of adherends recessing in SLJ with a brittle adhesive under tensile loading. They used experimental and numerical approaches to optimise recess dimension for different values of overlap length to achieve maximum joint strength.

Material modification aims to optimise the stiffness of the adherend and adhesive to decrease stress concentration at the overlap edges. One of these approaches includes the utilisation of mixed-adhesives along the bonding area by using higher stiffness adhesive in the mid-section of the adhesive and low stiffness adhesives at the edges. In this technique, the flexible adhesives provide more uniform stress distribution in the single-lap joint by transmitting large amounts of the load into mid-section of the overlap, which leads to smaller stress concentration at the overlap edges and higher joints strength [3] [14]. Da Silva and Lopes [15] used the same method, by applying brittle adhesive (high stiffness) in the inner region of the overlap and using three different ductile adhesives at the end of the overlap. Their results showed that the SLJ with ductile adhesive has lower strength than the one with brittle adhesive and the mixed-adhesive joint has higher strength than the SLJs with mono adhesives. Öz and Özer [16] studied the effect of mixed-adhesives on the failure load of SLJ experimentally. They concluded that the SLJs with mixed-adhesive had higher failure load than the joints that used only one of the adhesives. The same authors [17] studied the stress distribution of a mixed-adhesive single-lap joint by comparing the analytical solution with a 3D finite element (FE) solution. The adhesive section modelled in three sections by using flexible adhesives at the outer region and high stiffness adhesive in the mid-section of adhesive. Bavi et al. [18] used Genetic Algorithms to optimise the geometry of the bond-line in mixed-adhesive single-lap and double-lap joints. Their results present excellent optimal cases when the best compromise exists between the weight and strength of the joint. The improper ratio of stiff and flexible adhesive in the mixed-adhesive bond-line alter peel stress from compressive to tensile, which leads to a secondary peak in the peel stress distribution [19].

There are several studies on the improvement of strength and stress distribution of single-lap joints with similar adherends, while few works have been carried to improve the performance of the single-lap joints with dissimilar adherends (hybrid joint). The difference in the stiffness of the adherends leads to asymmetric stress distribution along the bond-line with the higher shear stress concentration on the low stiffness adherend side [20]. The increased use of hybrid joints such as bonding composites to metals in aerospace, maritime and civil and transport structures in the past decades makes it essential to find a method to improve the performance of this type of joints.

The main objective of this work is to improve the performance of the joint with dissimilar adherends by using geometrical and material modifications. In order to do this, in the first section, novel designs introduced by using notches along the bond-line to reduce stress concentration at the edges for an epoxy adhesive with similar adherends. Then the optimum design from the first section is used for single-lap joints with dissimilar adherends by using mono and mixed-adhesives to optimise the hybrid joints. The FE method has been utilised to understand the effect of the geometrical and material changes in the peak stresses at the overlap edges. Moreover, experimental tests are conducted to verify the strength improvement of each modification.

2. Experiment

2.1 Material Selection

Two adherends and adhesives materials were used in this work with the material properties shown in Table 1. Terson MS 9399 and Loctite EA 9497 have been used as polyurethane and epoxy adhesives, respectively. Loctite EA 9497 is a two-component room temperature curing epoxy of medium viscosity, while Teroson MS 9399 is a highly viscous, sag-resistance two-component polyurethane adhesive based on silane-modified polymers. The adherends were cut from aluminium alloy 6082 T6 bar and Polyphthalamide (PPA) plates. PPA is commercially called Grivory HTV-5H1 black 9205, made of 50% glass fibre reinforced engineering thermoplastic material based on a semi-crystalline, partially aromatic polyamide. The material properties were obtained from previous research through tensile tests based on ISO EN 485-2:2004 standard for adherends, and ISO 37 and ISO 527-2 for polyurethane and epoxy adhesives, respectively.

Table 1: The bulk property of adherends and adhesives

Property	Aluminium 6082 T6	Polyphthalamide	Terson MS 9399	Loctite EA 9497
Young Modulus (MPa)	70770 ± 380	17620 ± 600	3.06 ± 0.21^{a}	7705.35 ± 468.08
Yield Stress (MPa)	254.59 ± 3.20	241.33 ± 10.4	2.56 ± 0.13	46.29 ± 3.13
Elongation at fracture (%)	10.83 ± 0.95	1.71 ± 0.04	153.03 ± 14.38	0.71 ± 0.09
Poisson Ratio	0.30 ± 0.01	0.32 ± 0.04	0.44 ± 0.01	0.29^{b}
Density (tonne/m^3)	2.7^{b}	1.65^{b}	1.4^{b}	1.1^{b}

[a] Estimated from Neo-Hooken method [b] Manufacturer data

2.2 Joint configuration and fabrication

In this study, five different types of single-lap joints were manufactured, which are the unmodified configuration of SLJ (without notches); (Figure 1 a) and with the different number of notches in the adherend along the bonding area (Figure 1 b). In order to have a better discussion, all these joints are labelled as follows: Unmodified (Model-0), with two notches (Model-2), three notches (Model-3), four notches (Model-4) and five notches (Model-5).

All five types of SLJs were manufactured with identical values of grip-grip separation points ($L_t = 121$ mm), the thickness of adherends ($t_s = 3$ mm), the thickness of the adhesive ($t_A = 0.2$ mm) and joint's width ($w = 25$ mm) and the overlap length of ($L_s = 29$ mm). The tabs with a dimension of $L_{TAB} = 25$ mm were bonded at the end of the joints to secure correct alignment in the testing machine. Classic single-lap joint (Model-0) without any modification was used as the reference model to compare stress distribution and strength with the modified SLJs to understand the advantage of the notching technique in the bonding area. The manufacturing of the specimens started by cutting aluminium plaques using the hydraulic guillotine to the desired dimensions. The CNC machine with a 2 mm ball nose cutter was used to create notches with a depth of 0.5 mm along the bonding area.

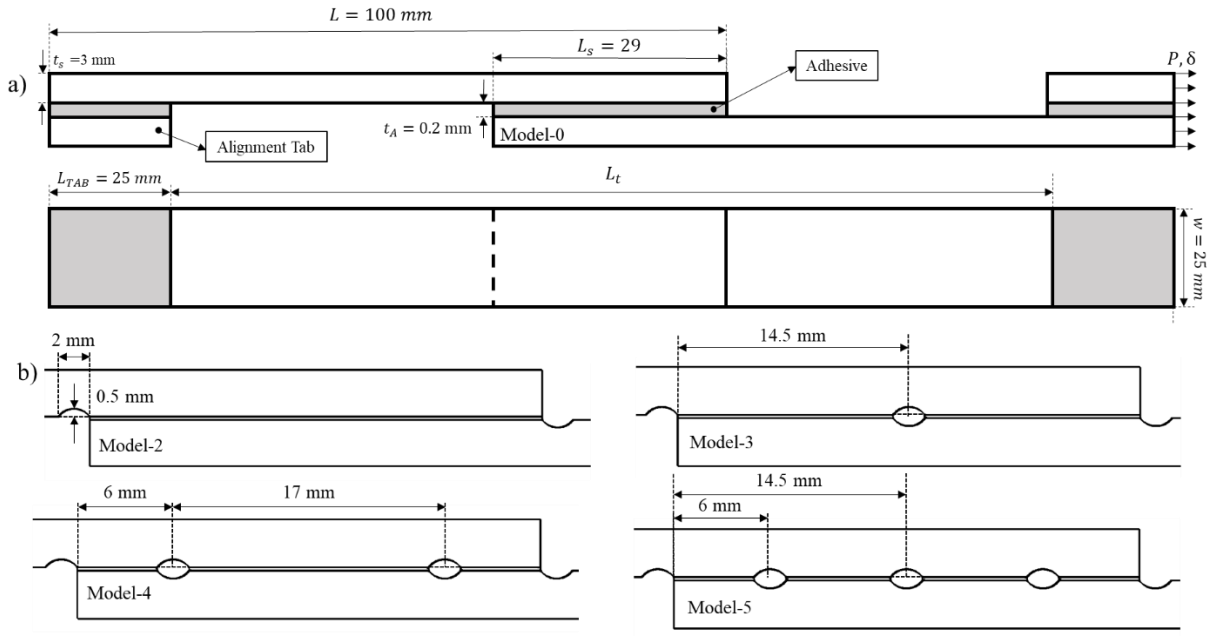

Figure 1: Dimensions and geometry of SLJs (a) unmodified (without notches) (b) with notches

Table 2 shows the number of notches and the total bonding length for each joint design. The first two notches are located outside the overlap area at both edges, and by adding more notches, the bonding length decreases as each notch removes 2 mm of the bonding surface.

Table 2: Joint configurations tested for optimisation purposes

ID	Total Bonding length (mm)	Number of notches in the bonding area
Model-0	29	0
Model-2	29	2
Model-3	27	3
Model-4	25	4
Model-5	23	5

The same surface treatment was carried out for all types of SLJs to increase the bonding strength. The bonding surface was grit blasted and then cleaned first with compressed air to remove dust created during the blasting process, followed by Acetone and Loctite SF 706 to remove grease spots. The curing process of the adhesives was done at room temperature by applying pressure with spring clamps for seven days to reach the fully cured strength. Wire spacers, with a diameter of 0.2 mm, were used to control bond-line thickness. The excess adhesive at the holes of the modified SLJs and the overlap ends were removed to provide identical conditions for all tested specimens.

The tensile tests were carried out with Instron 3380 series machine with 100 kN load cell at room temperature under displacement control of 0.5 mm/min. The non-contact optical method (Imetrum system) was used to measure displacement and observe the failure process in joints (Figure 2). All specimens were masked with white background and marked with black dots with a diameter of 0.3 mm in order to create speckle patterns on the specimens' surface. The camera then tracked the dots and the

first pattern was used as the reference image, to which other images were compared. When calibrating the dimension for the camera, the paper rule was used.

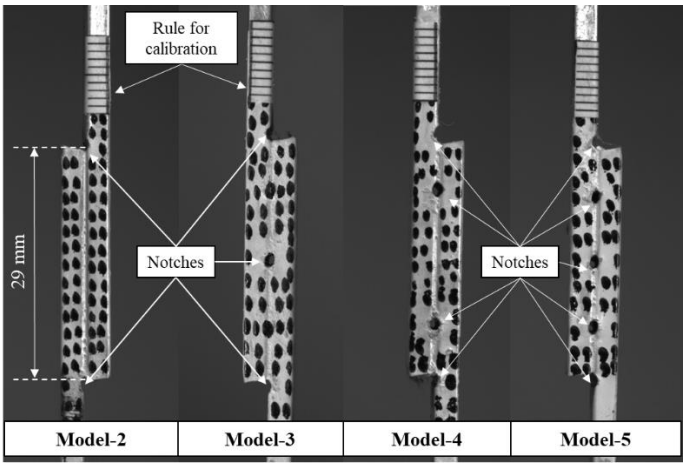

Figure 2: The geometry of single-lap joints with notches

3. Finite element analysis

The two dimensional (2D) nonlinear numerical models of modified and unmodified single-lap joints with different adherends and adhesives were built in Abaqus® to provide information regarding stress distribution, failure process, and joint strength. 2D (plane strain) model provides a reasonable simplification of the 3D model for the bonded joint [21]. In the first place, the aim of the finite element analysis (FEA) is to find the best pattern of notches along the bond-line for the SLJ and then optimise the SLJ with dissimilar adherends (Hybrid joint) by considering the selected notched design and using both mono-adhesive and mixed-adhesives.

The explicit non-linear analyses were used to simulate the rapid crack growth along the bond-line of the epoxy adhesive and the large deformation and distortion, especially for the polyurethane adhesive. Two different cases were analysed. Case-1 used a cohesive zone model (CZM) to predict joints' strength and Case-2 used only for stress analysis along the bond-line without including any damage parameters (CZM property) of adhesives. In the Case-1, the adherends were meshed by 4-noded plane-strain elements (CPE4R in ABAQUS) with four elements in the thickness direction. Mesh size of 0.2 mm along the length was finally chosen after a mesh convergence study.

The adhesive section was divided into three layers; two layers of cohesive elements (COH2D4) of 0.05 mm thick each located adjacent to the adherends and one layer of plan strain element (CPE4R) of 0.1 mm thick in the middle of the bond-line (Figure 3). Here, paths 1 and 2, respectively simulated interactions between the adhesive and adherends 1 and 2 by using interface properties between the adherends and the adhesives. The interface properties include elasticity, plasticity and susceptibility to damage, which can all change based on the combination of adherends in the joints. Table 3 shows the CZM parameters obtained in the previous research from the AL-AL and the PPA-PPA single-mode coupon tests for both adhesives. The nominal traction stress consists of two components, namely: t_n in

the normal direction and t_s in the shear direction, and these allow the simulation of damage initiation along the bond-line. The G_{IC} and G_{IIC} values represent the areas under the traction separation law graphs in the normal and shear directions, respectively [22].

For identical adherends SLJ, similar CZM property is used for path-1 and path-2 as the top and bottom adherends were made of identical materials. However, in the dissimilar SLJ path-1 and path-2 properties changes based on the adherend type. In this work, dissimilar SLJ is made of the AL (adherend-1) and the PPA (adherend-2) for all different designs. Path-1 has the properties of the AL-adhesive interface, and Path-2 has the PPA-adhesive interface properties (Table 3). The adherends and middle part of the adhesive used the bulk material properties from Table 1.

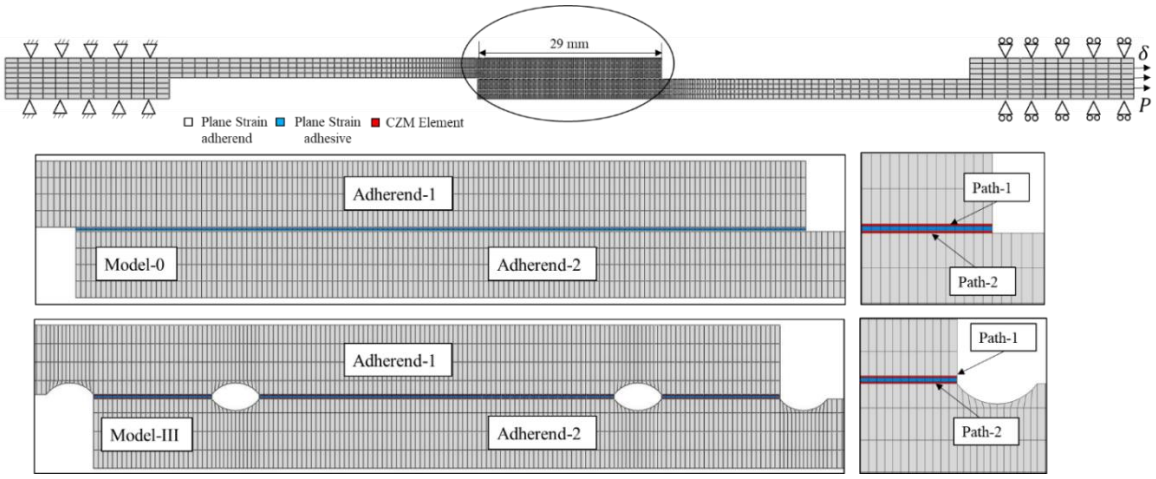

Figure 3: Mesh details for unmodified and modified SLJ with $L_s = 29\ mm$ for the case-1

A refined mesh scheme was used for the case-2 models to obtain a more accurate stress gradient at the edges [23]. The bonding area in the adhesive and the adherends were meshed with 4-noded plane-strain elements of $0.05\ mm \times 0.05\ mm$, and single bias effect were used in other part of adherend with minimum and maximum elements size of 0.05 and 0.2 mm, respectively.

Table 3: CZM parameters for two adhesives bonded with two different types of adherends

Interface Property	Terson MS 9399 (AL-Adhesive)	Terson MS 9399 (PPA-Adhesive)	Loctite EA 9497 (AL-Adhesive)	Loctite EA 9497 (PPA-Adhesive)
G_{Ic} (N/mm)	2.11 ± 0.27	0.95 ± 0.12	0.26 ± 0.06	0.22 ± 0.04
G_{IIc} (N/mm)	6.50 ± 0.20	4.10 ± 0.50	0.90 ± 0.388	0.46 ± 0.090
t_n (MPa)	2.52 ± 0.45	0.65 ± 0.24	25.35 ± 10.263	20.94 ± 7.27
t_s(MPa)	6.67 ± 0.25	3.50 ± 0.20	16 ± 5	10 ± 3.75

Due to the high viscosity of polyurethane adhesive, the hyper-elastic property was used to reduce mesh distortion caused by large deformation (Table 4).

Table 4: Arruda-Boyce parameters for polyurethane

Mu (MPa)	mu-0(MPa)	LAMBDA	D (MPa^{-1})
1.016	1.04	1867.76	0.152

4. Geometric modification results for SLJ with similar adherends

4.1 Stress analysis of un-notched and notched joints

The first aim of this research is to assess the effect of notches, located in the bonding area, on the behaviour of the single-lap joint. This was done by using the FE model in Abaqus® software to simulate a series of SLJ with various notch designs and to find the optimum one. The objective of the proposed designs is to reduce stress concentration at the edges, which can be more beneficial for epoxy adhesive as the bond-line edges play a significant role in carrying the external load [24] compared to flexible and ductile adhesives. Therefore, the epoxy adhesive was selected as the adhesive for the optimisation process. Moreover, aluminium was selected as the adherend in this section due to its higher stiffness compared to the PPA, which less likely experiences plastic deformation or failure under high tensile load. All the plots are the elastic stresses in the middle of the adhesive layer, which are normalised by the average shear stress in the adhesive bond-line of each design (Figure 4). The stress results obtained from an integration point of the element, which is the average value of the stress from four nodes in 2D-hex elements. The varying points along the bond-line (x) have also been normalised using the total overlap length (L_s).

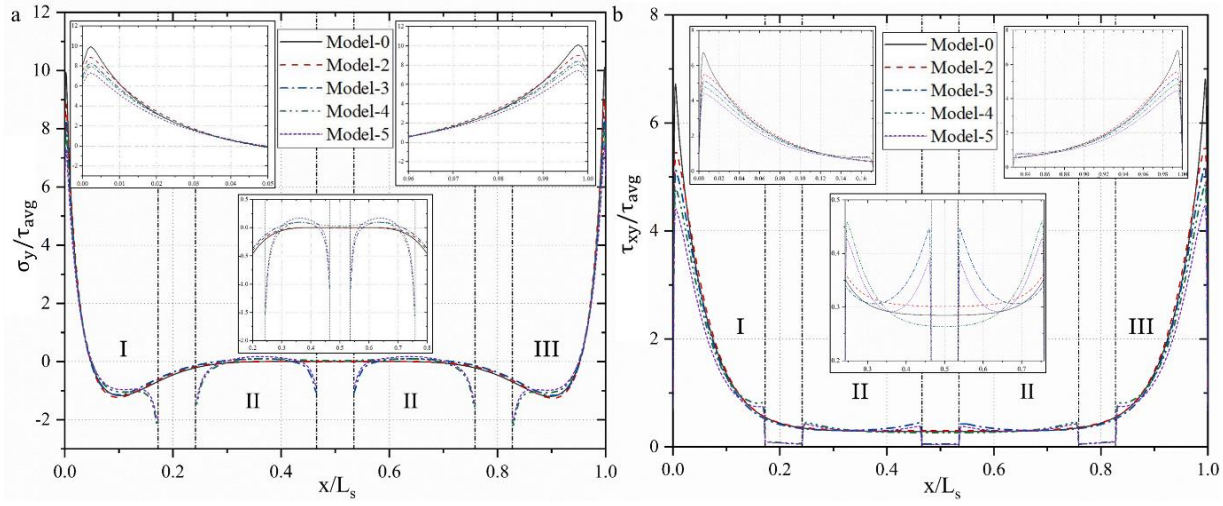

Figure 4: The comparison of (a) the peel (σ_y/τ_{avg})and the shear (τ_{xy}/τ_{avg}) stresses at the adhesive mid-thickness for different modified SLJs

As seen in Figure 4(a), the peel stress is more uniform in the mid-section of the overlap with higher stress concentration at the edges, which is caused by adherends rotation [25]. The shear stress follows an identical trend (Figure 4(b)), with lower stress at mid-section of the bond-line and the higher peak stresses at the edges due to the material discontinuity of the adherends at the free edges[26]. The magnitude of the peak σ_y/τ_{avg} and the peak τ_{xy}/τ_{avg} for unmodified single-lap joint (Model-0) at Section-I are 9.94 and 6.8, respectively, highest among all the models.

However, it is clear that the peak stresses at the edges of the overlaps of SLJs with notches (Model-2, Model-3, Model-4, and Model-5), are considerably lower than the unmodified SLJ (Model-0). The peak value of the σ_y/τ_{avg} decreases from 10.11 in Model-0 to 9.03 in Model-2, which corresponds to a

reduction of 10.6 %, and is due to the increase of the adherends' flexibility [13]. By increasing the number of notches along the overlap, the σ_y/τ_{avg} value exhibits further reduction of 16.7%, 20.0% and 26.4 %, respectively, for Model-3, Model-4 and Model-5 when compare to Model-0. The existence of notches along the overlap length divides the overlap area to smaller sections, which assists the modified SLJs to distribute the load more efficiently between each section. The peak value of the τ_{xy}/τ_{avg} follows the same tendency and decreases by 20.5% from 6.82 in Model-0 to 5.41 in Model-2. The τ_{xy}/τ_{avg} value at section-I experienced a further reduction of 23.9 % for Model-3, 28.9% for Model-4 and 34.5% for Model-5 when the number of notches increased in bond-line (Table 5).

Table 5: The maximum τ_{xy}/τ_{avg} and σ_y/τ_{avg} at the overlap edges for various SLJs designs

	Section-III			
ID	$\tau_{xy/\tau_{avg}}$ **(Peak)**	**Reduction (%)**	$\sigma_{y/\tau_{avg}}$ **(Peak)**	**Reduction (%)**
Model-0	6.82	-	10.11	-
Model-2	5.41	20.5	9.03	10.6
Model-3	5.17	23.9	8.42	16.7
Model-4	4.83	28.9	8.08	20.0
Model-5	4.45	34.5	7.44	26.4

In the mid-section of the overlap, Model-0 and Model-2 have the smoothest peel and shear stress distribution with the minor peak of -0.44 τ_{avg} at the mid-section ($0.2 < x < 0.8$) of the bond-line. On the other hand, the τ_{xy} and σ_y do not show a uniform stress distribution at the mid-section of the single-lap joints with notches due to the existence of free edges. The comparison of Model-0 and Model-5 shows that the peak value of stresses increased from -0.5 in Model-0 to -1.5 in Model-5 for the σ_y/τ_{avg} and from 0.44 in Model-0 to 0.48 in Model-5 for the τ_{xy}/τ_{avg}. This happens as modified single-lap joints can transfer load from overlap edges to the mid-section of the adhesive due to the existence of notches, which leads to smaller peak stress at the overlap edges. Therefore, from the stress analysis, it can be concluded that adding notches in the bonding area can improve the strength of single-lap joints.

4.2 Strength analysis of the un-notched and notched joints

In this section, the influence of various notch designs on the strength of single-lap joints is studied experimentally. Four specimens of each design are tested under tensile loading. Figure 5 shows the average failure load and the joint strength with standard deviation. The results in the previous and the following sections are used to select the best candidature design for the optimisation of single-lap joints with dissimilar adherends. Figure 5(a) shows that the average maximum failure load of Model-2 is improved by 6% compared to Model-0 (reference Model). This can be justified by the stress concentration reduction (20% and 10% for the τ_{xy}/τ_{avg} and the σ_y/τ_{avg}, respectively) at the edges due to the existence of the notches. Model-5 has experienced considerably smaller improvement of the

maximum failure load compared to Model-4 (around 2%) from 5026 N to 5082 N. This reflects the findings in Section 4.1 (Table 5), where the τ_{xy}/τ_{avg} and the σ_y/τ_{avg} of Model-5 were reduced only by 4% and 6%, respectively, in comparison to Model-4. Therefore, Model-4 is selected as an initially optimised design for further optimisation in the next section for dissimilar single-lap joints.

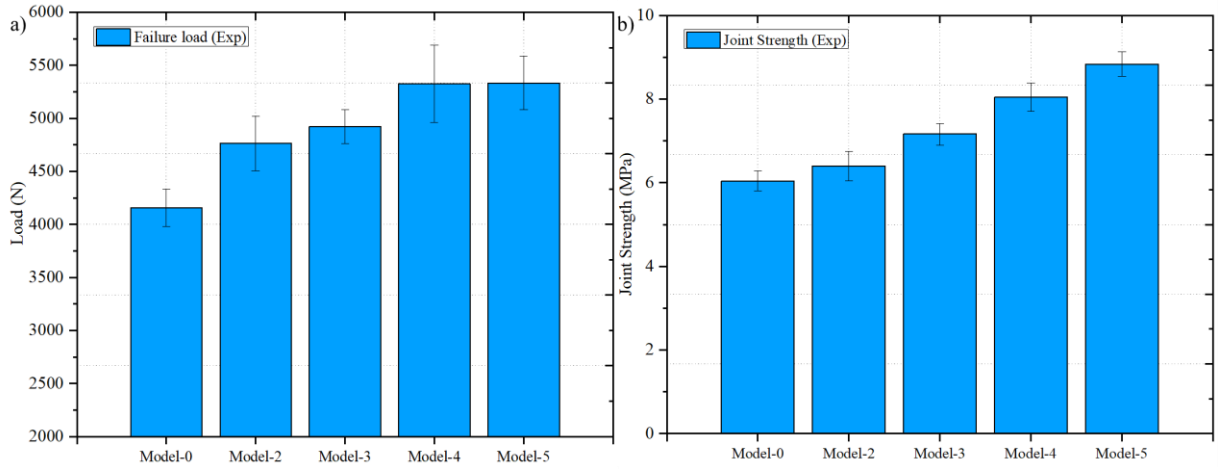

Figure 5: (a) average failure load and (b) average shear strength of various SLJs

As seen in Figure 5(b), the joint strength of Model-4 and Model-5 are 8.03 MPa and 8.83 MPa, respectively, which corresponds to an improvement of 30 % and 39% compared to the strength of Model-0 (5.95 MPa). This suggests that the modified SLJ with smaller bonding length could achieve higher strength and failure load. The above results demonstrate that the proposed design could improve the strength of the joints significantly by reducing peak stresses at the bond-line edges.

5. Optimisation of SLJ with dissimilar adherends

In this section, two types of designs are used with mono-adhesives (epoxy or polyurethane) and mixed-adhesive (Combination of epoxy and polyurethane) to optimise the performance of dissimilar single-lap joints. The fabrication process is the same as joining similar adherends in section 2.2. The optimisation process starts with comparing the AL-AL joint (Model-0) with the AL-PPA joint (Model-I) bonded with epoxy adhesive to understand the effect of individual adherend stiffness on the SLJ strength. Then the best design from section 4.2 (Model-4: SLJ with four notches) is used to increase the strength of the dissimilar single-lap joint by using mono-adhesives and mixed-adhesives.

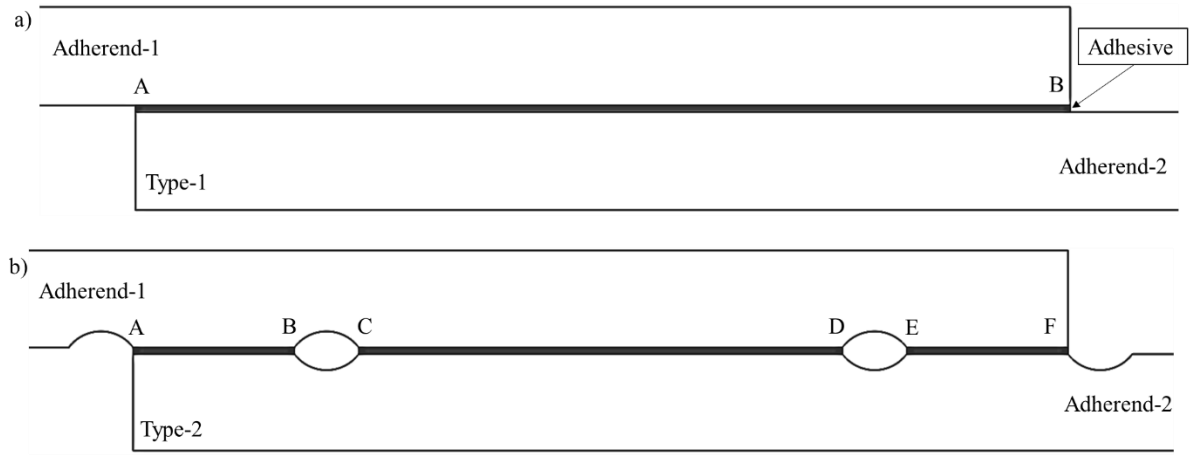

Figure 6: The SLJs configurations used for the optimisation process ((a) Classic SLJ and (b) Novel SLJ designs)

Table 6 shows adherends/adhesives and design type of single-lap joints to be used in the optimisation process. In total, six different types of SLJ are manufactured, which can be categorised into two groups un-modified (type-1) and modified (type-2) SLJs (Figure 6). Model-I and Model-II are using a classic single-lap joint design (type-1), which are used as the reference models for epoxy and polyurethane adhesives, respectively. Model-III, Model-IV, and Model-V are using the novel optimum design (type-2) from the previous section.

Table 6: Material and design types of single-lap joints

ID	Design type	Adherend-1	Adherend-2	Adhesive (A-B)	Adhesive (C-D)	Adhesive (E-F)
Model-0	1	AL	AL	Epoxy	-	-
Model-I	1	AL	PPA	Epoxy	-	-
Model-II	1	AL	PPA	Polyurethane	-	-
Model-III	2	AL	PPA	Epoxy	Epoxy	Epoxy
Model-IV	2	AL	PPA	Polyurethane	Polyurethane	Polyurethane
Model-V	2	AL	PPA	Polyurethane	Epoxy	Polyurethane

The bonding area in the type-2 design has three separate sections, which are named as A-B, C-D, and E-F. Mono-adhesives are used for Model-III (Epoxy adhesive) and Model-IV (Polyurethane adhesive) along bond-line while the combination of epoxy in the middle part (C-D) and polyurethane at the edges (A-B and E-F) are utilized for Model-V. In previous work by researchers [15] [16], silicon spacer used to separate adhesives from each other while the proposed design provides free space along the length of the overlap due to the existence of notches, which avoid mixing adhesives in the bonding area.

5.1 Stress analysis of dissimilar joints

This section presents the interfacial peel stress (σ_y) and shear stress (τ_{xy}) of the proposed design to find the influence of using notches and mix-adhesive in the bonding area on the stress distribution of the dissimilar single-lap joint. Numerical models were built in Abaqus® software for the joints shown in Table 6. All the FE parameters are kept the same as used for section 4.1 for all the models. Comparing the stress distribution of Model-0 (shown in Figure 4) and Model-I (shown in Figure 7) shows that Model-0 provides flatter peel stress at the inner overlap section. This can be explained by the less

flexibility of the AL-AL adherends compared to the AL-PPA, which leads to more uniform stress distribution and lower peak stresses at the overlap edges.

The asymmetric stress distribution is noticed in the SLJs with dissimilar adherends due to the mismatching stiffness of the adherends and boundary conditions in the two grip ends of two adherends, which results in different longitudinal deformations at the overlap edges. In Model-I, the maximum peak value of the τ_{xy}/τ_{avg} in section-III (PPA side) is higher by 130 % compared to section-I (AL side). This suggests that in a joint with dissimilar adherends, the adherend with lower stiffness controls the strength of the whole joint [20]. On the other hand, the σ_y/τ_{avg} shows smaller peak values in section-III due to the increase of the longitudinal deformation of the PPA adherend. Since the aluminium adherend experiences smaller longitudinal deformation, the higher peak value of the σ_y/τ_{avg} is developed toward section-I.

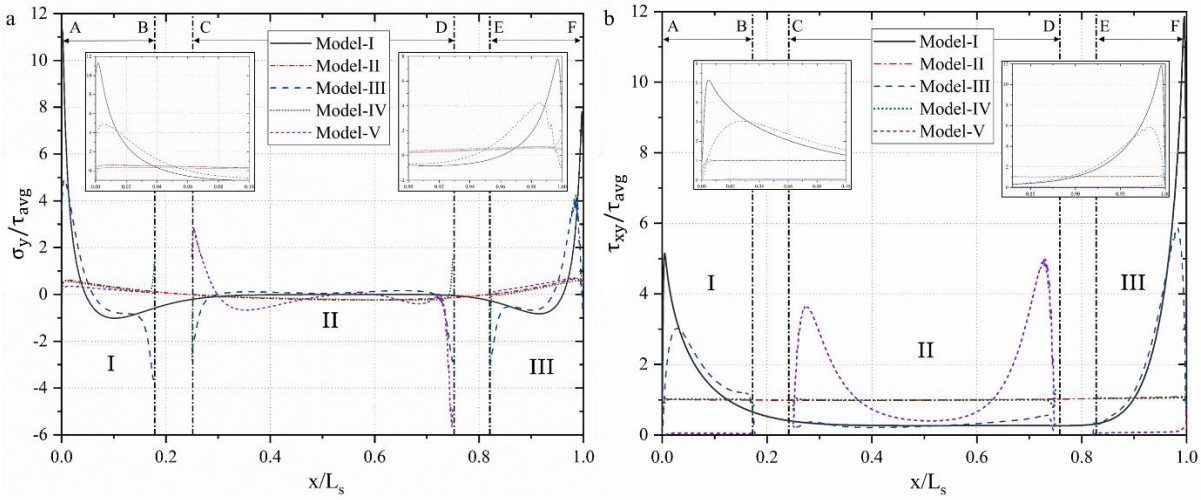

Figure 7: The comparison of (a) the peel (σ_y/τ_{avg}) and (b) the shear (τ_{xy}/τ_{avg}) stresses at the adhesive mid-thickness for different modified dissimilar SLJs

As seen in Figure 7, Model-III experiences a significant improvement in peak stresses at the overlap edges when compared with Model-I. The maximum peak value of the τ_{xy}/τ_{avg} decreases from 5.14 in Model-I to 3.05 in Model-III at section-I (AL side) and 11.85 in Model-I to 5.05 in Model-III at section-III (PPA side), which corresponds to a reduction of 40 % and 57%, respectively. The same tendency was observed for the σ_y/τ_{avg}, with a 50% and 53 % reduction of the peak stresses at section-I and section-III respectively, when compared with Model-I. In addition, the differences between the peak stresses at both overlap edges decrease from 30% in Model-I to 26% in Model-III for the σ_y/τ_{avg} and from 130% in Model-I to 65% in Model-III for the τ_{xy}/τ_{avg}. This suggests a smaller asymmetric stress distribution along the bond-line, which may lead to an improvement of the joint strength.

The polyurethane adhesive provides more uniform stress distribution along the bond-line compared to the epoxy adhesive due to its more significant deformation and load-transferring capacity. The comparisons of Mode-II and Model-IV show minimal improvement (5% reduction) of the peak stress

values at the bond-line edges. This can be justified by higher plasticisation of the polyurethane adhesive, which makes them less sensitive to the peak load at the overlap edges.

In the joint with mixed-adhesive (Model-V), the peak stresses at the overlap edges are slightly lower in comparison to the joints with mono-adhesive (Model-III). Moreover, the stress concentration is transferred into the interior part (C-D) of the overlap length. This suggests that the mixed-adhesive SLJ may have slightly higher strength when compared to the joints with mono adhesive. Consequently, crack initiation may occur in the mid-section of the overlap (C-D section) due to the higher stress concentration in the areas.

5.2 Load-displacement of dissimilar SLJs

In this section, the effect of adherends/adhesive stiffness, mixed-adhesives, and notches in the bonding area are studied both numerically and experimentally. The proposed modified single-lap joints (Model-III, Model-IV, and Model-V) were tested in identical conditions to optimise the configuration of the SLJ with dissimilar adherends.

As it is clear from Figure 8 (a), the failure load of SLJ with epoxy adhesive decreases by 13.1 % from 4115 N to 3574 N after changing the adherends combination from the AL-AL (Model-0) to the AL-PPA (Model-I). This happens due to the reduction of overall stiffness of the joint, which is caused by the lower stiffness of the PPA, resulting in larger bending, longitudinal deformation, and asymmetric stress distribution along the bond-line as it was discussed in section 5.1. The higher peak stresses at the lower stiffness adherend are important as it is likely that crack initiates at this location, especially if the adhesives are brittle, which are more sensitive to the stiffness of the adherends due to the higher peak stresses and instability in damage propagation [27].

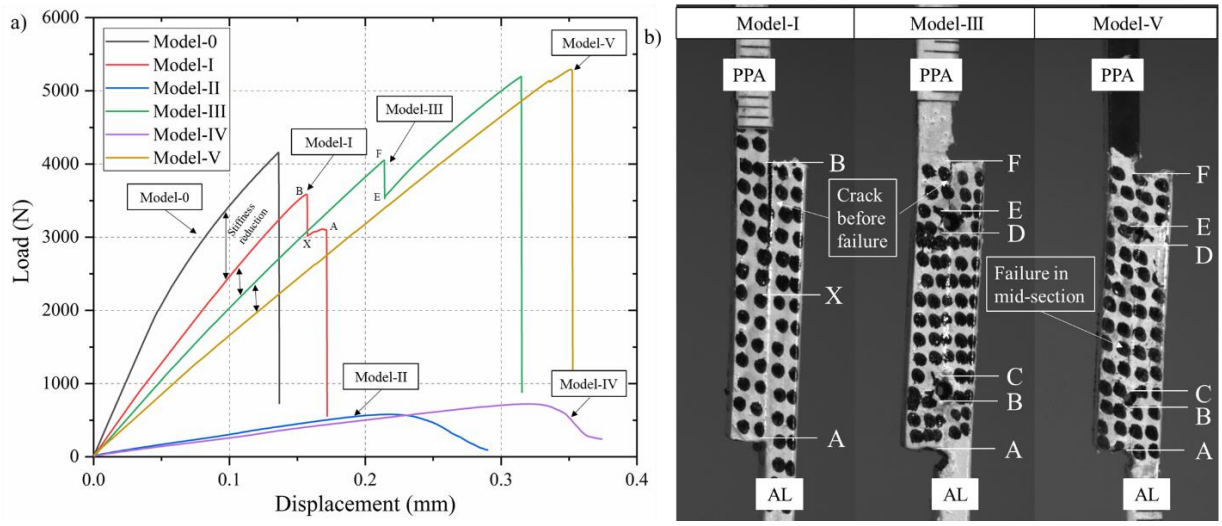

Figure 8: a) load-displacement of modified and unmodified SLJs b) failure process of SLJs

As can be seen from Figure 8 (b), in Model-I, the initial crack starts at the PPA-adhesive's interface (from B to X), followed very quickly by the total failure of the joint. This is due to the nature of the

brittle adhesives that do not tolerate plasticisation or stress redistribution after reaching failure strength at the overlap edges [24].

On the other hand, Model-III with epoxy adhesive experiences the first crack at 4048 N, which is 13.26% higher than Model-I, and only 1.62% lower than Model-0. This is due to the existence of the notches at the overlap edges, which reduces peak stresses at these locations (as shown in Figure 7). Moreover, the modified design with notches arrests cracks in section E-F without propagating the crack further into other parts of the bond-line (D-E and B-A). Therefore, this model can redistribute the stresses in sections D-E and B-A and tolerates a maximum load of 5194.7 N, which is 26% and 45% higher than model-0 and Model-I, respectively.

Model-IV with polyurethane adhesive experiences smaller improvement compared to the unmodified SLJ with polyurethane adhesive (Model-II). The maximum failure load increases from 578 N in Model-II to 715 N in Model-IV, which corresponds to a 23 % increase.

It can be noticed that the combination of the epoxy and polyurethane adhesives gives a higher failure load than when they are used as adhesives individually. The maximum failure load for Model-V is 5292 N, which is higher than that of Model-I and Model-II by 48% and 782 %, respectively. This can be explained by the smaller rotation of the polyurethane adhesive in the section (A-B and E-F), which leads to lower stress concentration at the edges (shown in Figure 7). Model-V fails in the mid-section (D-C) of the overlap as polyurethane adhesive transfers stresses to the mid-section that carries most of the load, though a slight drop before failure is observed, indicating plastic deformation in polyurethane adhesive.

The displacement at failure is increased by 30 % after changing the adherends combination from the AL-AL (Model-0) to the AL-PPA (Model-I). This can be justified by the lower stiffness of the PPA, which increases the overall longitudinal strain of the SLJ. In addition, adding notches to adherends decrease the total stiffness of the SLJ, resulting in higher flexibility of the joint. Model-V and Model-IV have the greatest displacement at the failure due to the existence of the polyurethane adhesive, which allows more extensive deformation in the bonding area before failure.

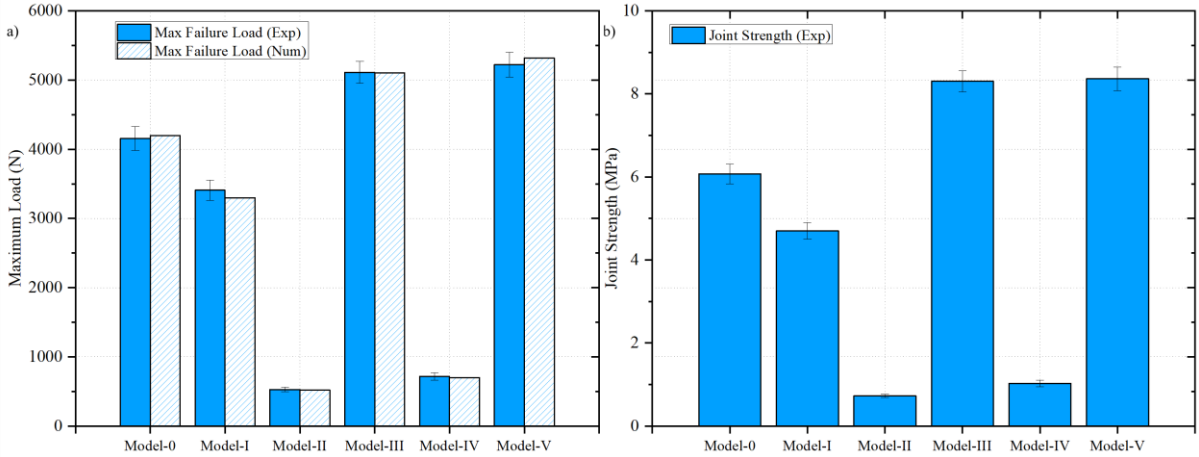

Figure 9: The comparison of (a) experimental and numerical failure load and (b) shear strength of various SLJs

Figure 9 (a) shows a good agreement regarding the maximum failure load between the numerical and the experimental results. The average experimental failure loads are obtained from four specimens, and the numerically predicted failure loads are obtained using the CZM method. It is clear from Figure 9 (b) that the unmodified joint with dissimilar adherends (Model-I) has a 22% smaller strength in comparison with the unmodified joint with similar adherends (Model-0), which is due to the decrease in total stiffness of the joint.

On the other hand, the proposed novel design increases the strength of the joints considerably. The strength of model-III is 8.3 MPa, which is 36 % and 76% higher when compared to Model-0 and Model-I, respectively. In addition, by utilising the mixed-adhesive in the bonding area, the strength of the joint increases slightly to 8.36 MPa. This design also has a positive effect on the joint with only polyurethane adhesive as the strength is increased by 41 % from 0.728 MPa in model-II to 1.028 MPa in Model-IV. In conclusion, the proposed novel design shows significant improvement in the performance of the SLJ with dissimilar adherends, which makes them significantly stronger than the SLJ joint with similar adherends.

5.3 Damage variable analysis

This section analyses the overall scalar stiffness degradation of the CZM elements along the bond-line to understand the failure process of various dissimilar single-lap joints under tensile loading. The damage variable (SDEG) value varies between 0 (undamaged) and 1 (fully damaged).

The numerical and experimental results show that the crack is initiated and propagated at the interface of the PPA for all types of single-lap joints with dissimilar adherends, which is in agreement with the previous study. Therefore, the SDEG is plotted for path-2 (PPA side) as a function of (x/L_s) as the representative joint configurations. Figure 10 (a) shows the SDEG plots at the instant when the first CZM element fails and Figure 10 (b) is the SDEG plot under maximum load before failure.

As seen in Figure 10 (a), the crack is initiated for all models except Model-V at $x/L_s = 1$ (PPA side). This can be explained by the sensitivity of the epoxy adhesive to the high peak stresses at the edges caused by asymmetric stress distribution of the dissimilar joint (shown in Figure 7), leading to higher peak stresses at the overlap edges of the lower stiffness adherend [20]. The crack is initiated in the mid-section of Model-V due to the existence of the polyurethane adhesive at the edges (A-B and E-F), which provides more uniform stress distributions at the edges and transfers the load to the mid-section of the adhesive layer. Moreover, the analysis shows smaller SDEG values for polyurethane adhesive compared to the epoxy adhesive. This is due to the lower strength of the polyurethane adhesive, leading to smaller tractions (t_n,t_s) and higher fracture energies (G_{Ic},G_{IIc}) in both directions (Table 3).

It is clear from Figure 10 (b) that Model-III has more widespread damage in comparison to Model-I. The percentage of the overlap under the damage of Model-III and Model-I are 80% and 64%, respectively. In Model-I, crack is initiated at the PPA side and fails shortly after reaching the maximum

failure load. This can be justified by the limited damage tolerance of the epoxy adhesive immediately after reaching stress softening in the damage law [27]. On the other hand, the novel design of Model-III stops the crack propagation into section D-A due to the existence of the notches (D-E section), which allows the joint to redistribute the load into the mid-section of the adhesive layer, leading to a higher failure load.

The comparison of Model-II and Model-IV shows the same trend for the joints with only polyurethane adhesive. The novel single-lap joint design (Model-IV) with notches improves the SDEG value before failure, mostly in the mid-section of the adhesive from 0.15 to 0.31 when compared to Model-II. In addition, The SDEG plot of Model-II is unsymmetrical, while significant improvement is observed from Model-IV, where more uniform damage area is found along the overlap.

The total length of damage in the overlap length for Model-V is 91%, highest among all the models. This is due to the higher longitudinal strain of the polyurethane adhesive, resulting in more uniform stress distribution in the bond-line [28]. Moreover, the asymmetric behaviour of SDEG caused by the difference in the stiffness of the adherends was improved slightly for Model-V.

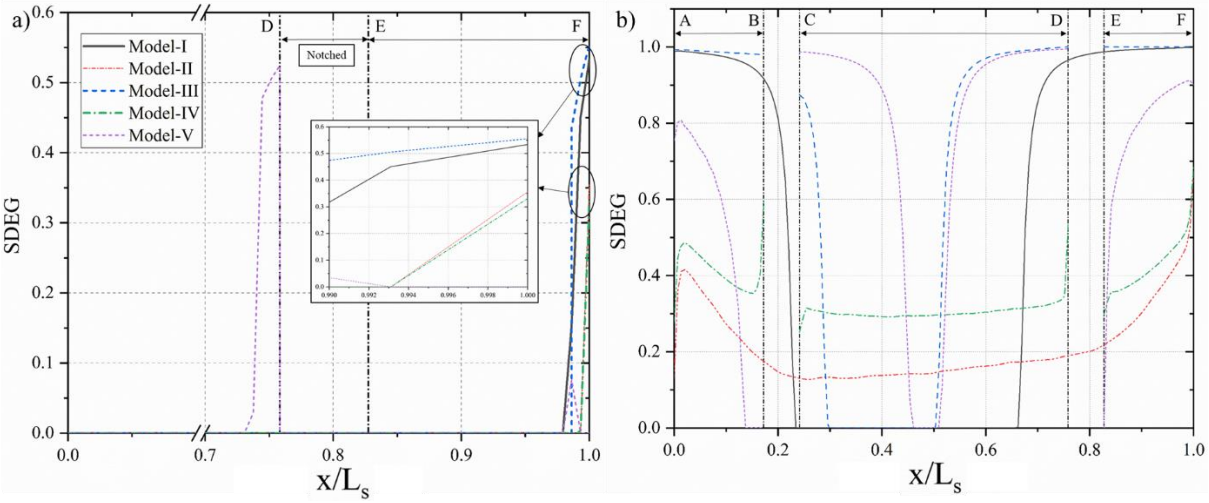

Figure 10: SDEG plot of unmodified and modified dissimilar single-lap joint (a) when the first CZM element damaged (b) under the maximum load point before joint failure

6. Conclusion

In this work, the effect of geometrical and material modifications on the strength and maximum failure load was studied. Geometrical modifications by adding notches along the overlap length were used first for joints with similar adherends and epoxy adhesive to find the optimum design. The chosen design was used next for single-lap joints with dissimilar adherends with mono and mixed-adhesives to optimise hybrid joints. The following observations have been found from experimental and numerical results:

- The stress-distribution of the SLJs with similar adherends and epoxy adhesive demonstrates that the peak stresses at the overlap edges of an SLJ with notches (Model-2, Model-3, Model-

4 and Model-5), are considerably lower than the unmodified SLJ (Model-0). The existence of notches along the overlap length divides the overlap area to smaller sections, which assists the modified SLJs to spread the load more efficiently between each section, leading to smaller peak stresses at the edges.

- In comparison with the un-modified SLJs, the strength and maximum failure load of the modified SLJs with similar adherends and epoxy adhesive shows significant improvement.
- Modified SLJs with smaller bonding length can achieve higher strength and failure load than unmodified SLJs with longer bonding length. This suggests that joints with epoxy adhesives experience smaller improvement by increasing the overlap length due to their vulnerability to high peak stresses.
- The load-displacement result of the unmodified dissimilar SLJ shows that the joint is failed very quickly after the crack initiation. The reason is the high peak stresses at the edges due to the difference in the stiffness of adherends, leading to asymmetric stress distribution. On the other hand, the novel design of dissimilar joints can carry a higher maximum failure load as the notches arrest crack and allow stress distribution in other sections of the adhesive layers, resulting in a higher strength of the joint.
- The SDEG plots show that the geometrical modification cannot reduce or eliminate asymmetric stress distribution in the dissimilar SLJs caused by the difference in the stiffness of adherends. However, the asymmetry of the stresses becomes less obvious as the number of notches increases, e.g., in Model-V, which leads to improvement in joint strength.

References

[1] R. B. Heslehurst, "Observations in the structural response of adhesive bondline defects," *Int. J. Adhes. Adhes.*, vol. 19, no. 2–3, pp. 133–154, Apr. 1999.

[2] M. K. Apalak and A. Engin, "An investigation on the initiation and propagation of damaged zones in adhesively bonded lap joints," *J. Adhes. Sci. Technol.*, vol. 17, no. 14, pp. 1889–1921, Jan. 2003.

[3] I. Pires, L. Quintino, J. F. Durodola, and A. Beevers, "Performance of bi-adhesive bonded aluminium lap joints," *Int. J. Adhes. Adhes.*, vol. 23, no. 3, pp. 215–223, Jan. 2003.

[4] M. K. Apalak and A. Engin, "Effect of adhesive free-end geometry on the initiation and propagation of damaged zones in adhesively bonded lap joints," *J. Adhes. Sci. Technol.*, vol. 18, no. 5, pp. 529–559, Jan. 2004.

[5] F. J. P. Chaves, L. F. M. da Silva, and P. M. S. T. de Castro, "Adhesively bonded T-joints in polyvinyl chloride windows," *Proc. Inst. Mech. Eng. Part L J. Mater. Des. Appl.*, vol. 222, no. 3, pp. 159–174, Jul. 2008.

[6] R. D. Adams, R. W. Atkins, J. A. Harris, and A. J. Kinloch, "Stress Analysis and Failure Properties of Carbon-Fibre-Reinforced-Plastic/Steel Double-Lap Joints," *J. Adhes.*, vol. 20, no. 1, pp. 29–53, Jul. 1986.

[7] E. Sancaktar and P. Nirantar, "Increasing strength of single lap joints of metal adherends by taper minimization," *J. Adhes. Sci. Technol.*, vol. 17, no. 5, pp. 655–675, Jan. 2003.

[8] A. S. McLaren and I. MacInnes, "The influence on the stress distribution in an adhesive lap joint of bending of the adhering sheets," *Br. J. Appl. Phys.*, vol. 9, no. 2, pp. 72–77, Feb. 1958.

[9] R. D. S. G. Campilho, A. M. G. Pinto, M. D. Banea, R. F. Silva, and L. F. M. da Silva, "Strength Improvement of Adhesively-Bonded Joints Using a Reverse-Bent Geometry," *J. Adhes. Sci. Technol.*, vol. 25, no. 18, pp. 2351–2368, Jan. 2011.

[10] J. Y. Cognard, R. Créac'hcadec, and J. Maurice, "Numerical analysis of the stress distribution in single-lap shear tests under elastic assumption—Application to the optimisation of the mechanical behaviour," *Int. J. Adhes. Adhes.*, vol. 31, no. 7, pp. 715–724, Oct. 2011.

[11] E. Sancaktar and S. R. Simmons, "Optimization of adhesively-bonded single lap joints by adherend notching," *J. Adhes. Sci. Technol.*, vol. 14, no. 11, pp. 1363–1404, Jan. 2000.

[12] Z.-M. Yan, M. You, X.-S. Yi, X.-L. Zheng, and Z. Li, "A numerical study of parallel slot in adherend on the stress distribution in adhesively bonded aluminum single lap joint," *Int. J. Adhes. Adhes.*, vol. 27, no. 8, pp. 687–695, Dec. 2007.

[13] A. M. G. Pinto, N. F. Q. R. Ribeiro, R. D. S. G. Campilho, and I. R. Mendes, "Effect of Adherend Recessing on the Tensile Strength of Single Lap Joints," *J. Adhes.*, vol. 90, no. 8, pp. 649–666, Aug. 2014.

[14] M. D. Fitton and J. G. Broughton, "Variable modulus adhesives: an approach to optimised joint performance," *Int. J. Adhes. Adhes.*, vol. 25, no. 4, pp. 329–336, Aug. 2005.

[15] L. F. M. da Silva and M. J. C. Q. Lopes, "Joint strength optimization by the mixed-adhesive technique," *Int. J. Adhes. Adhes.*, vol. 29, no. 5, pp. 509–514, Jul. 2009.

[16] Ö. Öz and H. Özer, "An experimental investigation on the failure loads of the mono and bi-adhesive joints," *J. Adhes. Sci. Technol.*, vol. 31, no. 19–20, pp. 2251–2270, Oct. 2017.

[17] H. Özer and Ö. Öz, "Three dimensional finite element analysis of bi-adhesively bonded double lap joint," *Int. J. Adhes. Adhes.*, vol. 37, pp. 50–55, Sep. 2012.

[18] O. Bavi, N. Bavi, and M. Shishesaz, "Geometrical Optimization of the Overlap in Mixed Adhesive Lap Joints," *J. Adhes.*, vol. 89, no. 12, pp. 948–972, Dec. 2013.

[19] H. Özer and Ö. Öz, "A Comparative Evaluation of Numerical and Analytical Solutions to the Biadhesive Single-Lap Joint," *Math. Probl. Eng.*, vol. 2014, pp. 1–16, 2014.

[20] P. N. B. Reis, J. A. M. Ferreira, and F. Antunes, “Effect of adherend’s rigidity on the shear strength of single lap adhesive joints,” *Int. J. Adhes. Adhes.*, vol. 31, no. 4, pp. 193–201, Jun. 2011.

[21] Y. Hua, A. D. Crocombe, M. A. Wahab, and I. A. Ashcroft, “Continuum damage modelling of environmental degradation in joints bonded with EA9321 epoxy adhesive,” *Int. J. Adhes. Adhes.*, vol. 28, no. 6, pp. 302–313, Sep. 2008.

[22] R. D. S. G. Campilho, M. D. Banea, J. A. B. P. Neto, and L. F. M. da Silva, “Modelling of Single-Lap Joints Using Cohesive Zone Models: Effect of the Cohesive Parameters on the Output of the Simulations,” *J. Adhes.*, vol. 88, no. 4–6, pp. 513–533, Apr. 2012.

[23] R. D. S. G. Campilho, M. F. S. F. de Moura, and J. J. M. S. Domingues, “Modelling single and double-lap repairs on composite materials,” *Compos. Sci. Technol.*, vol. 65, no. 13, pp. 1948–1958, Oct. 2005.

[24] J. O. S. Silva, R. D. S. G. Campilho, and R. J. B. Rocha, “Crack growth analysis of adhesively-bonded stepped joints in aluminium structures,” *J. Brazilian Soc. Mech. Sci. Eng.*, vol. 40, no. 11, p. 540, Nov. 2018.

[25] B. Zhao, Z. H. Lu, and Y. N. Lu, “Two-dimensional analytical solution of elastic stresses for balanced single-lap joints - Variational method,” *Int. J. Adhes. Adhes.*, 2014.

[26] W. Jiang and P. Qiao, “An improved four-parameter model with consideration of Poisson’s effect on stress analysis of adhesive joints,” *Eng. Struct.*, vol. 88, pp. 203–215, Apr. 2015.

[27] D. L. Alves, R. D. S. G. Campilho, R. D. F. Moreira, F. J. G. Silva, and L. F. M. da Silva, “Experimental and numerical analysis of hybrid adhesively-bonded scarf joints,” *Int. J. Adhes. Adhes.*, 2018.

[28] G. P. Marques, R. D. S. G. Campilho, F. J. G. da Silva, and R. D. F. Moreira, “Adhesive selection for hybrid spot-welded/bonded single-lap joints: Experimentation and numerical analysis,” *Compos. Part B Eng.*, vol. 84, pp. 248–257, Jan. 2016.